

# Photolytic Degradation of Methylene Blue: The Effect of Various Factors on Wastewater Treatment Efficiency

## ABSTRACT

In Ivory Coast, dyes are widely used in traditional textile dyeing. It's a lucrative business that is attracting more and more people. Unfortunately, the wastewater from these textile dyeing units is discharged directly and continuously into the immediate environment. This poses a risk to human health and the environment. Among these dyes, the frequently used methylene blue (MB) can disrupt the balance of aquatic ecosystems by affecting the survival of aquatic organisms, inhibit photosynthesis in exposed plants, and cause irritation or toxic effects in humans in the event of prolonged exposure. This work investigated the degradation of methylene blue (MB), a model dye, by photolysis. The effects of the following parameters were studied: initial dye concentration, pH, H<sub>2</sub>O<sub>2</sub>, NaI, NaCl, and NaCl combined with H<sub>2</sub>O<sub>2</sub> or NaI. The experiments were monitored using a UV-visible spectrophotometer. The results showed that MB can be effectively degraded by direct photolysis in a basic medium and at very low concentrations. Additionally, NaI and H<sub>2</sub>O<sub>2</sub> had a very significant positive effect (83.77 % and 92 %) in contrast to NaCl (6.23 %). Furthermore, the treatment of MB solution was enhanced when NaCl was combined with NaI or H<sub>2</sub>O<sub>2</sub> with a degradation rate of 88.1 and 84.9 %, respectively. The kinetic study revealed that the UV irradiation of MB can be described by both zero-order and first or second-order kinetics. In conclusion, the UV/H<sub>2</sub>O<sub>2</sub>, UV/NaI, UV/NaCl+H<sub>2</sub>O<sub>2</sub>, and UV/NaCl+NaI systems represent very interesting alternative processes for the treatment of wastewater containing dyes at neutral pH. These methods are particularly suitable for industries involved in textile dyeing and other activities generating dye-contaminated effluents, offering an efficient and environmentally friendly solution for mitigating water pollution and meeting regulatory standards.

*Keywords: Advanced oxidation process; Methylene Blue dye; inorganic ions; UV light*

## 1. INTRODUCTION

Dyes are aromatic organic compounds that absorb light and produce colour in the visible spectrum (Abd-Elhamid et al. 2020, Benkhaya et al. 2020). They are used in a variety of sectors, including the textile, pharmaceutical, and food industries. Unfortunately, a significant portion of these dyes is discharged daily into water bodies after use (Atta et al. 2024), contributing significantly to environmental pollution.

In Ivory Coast, traditional textile dyeing is a thriving informal sector that attracts an increasing number of people due to its financial benefits. Most artisans involved in this sector acquire their skills through family traditions passed down over generations or by learning from master artisans. However, artisans typically lack access to crucial information, such as the supplier,

28 country of origin, expiration date, usage guidelines, and the effects of dyes on human health  
29 and the environment. They are generally sold in simple plastic packaging and are handled by  
30 artisans without adequate protective measures, such as masks, gloves, or goggles. Moreover,  
31 wastewater from these dyeing activities is frequently discharged directly onto the ground or  
32 into the sewerage system without prior treatment, posing severe pollution risks to the  
33 environment and human health. The dyes used in this sector are known to be non-  
34 biodegradable, resistant to conventional methods of pollutant degradation, toxic, and with  
35 some being carcinogenic (Contreras et al. 2019, Sun et al. 2019). In addition, the discharge of  
36 dye-containing wastewater results in aesthetic pollution and eutrophication. This affects  
37 aquatic life by promoting excessive algae growth, **and** reducing oxygen levels required to  
38 sustain aquatic ecosystems (Lianmawii et Singh 2023). The dye effluents are also mutagenic  
39 and toxic to various microbiological and fish species (Lianmawii et Singh 2023)

41 Discovered by Heinrich Caro in 1878, methylene blue belongs to the group of quinone imides,  
42 section Thiazines, which are sulfur dyes in which two benzene rings are joined by a closed  
43 ring of one nitrogen atom, one sulfur atom and 4 carbon atoms. Methylene blue (MB) is a  
44 versatile molecule used in medicine to treat diseases such as malaria, anemia, Alzheimer's  
45 and certain infections. It is also used in phototherapy to treat cancer and to inactivate RNA  
46 viruses. In industry, it is used as a textile dye and chemical indicator, and has applications in  
47 solar cells, sensors and fuel cells (Mashkoo et Nasar 2020, Khan et al. 2022). However, MB  
48 is toxic, carcinogenic, and non-biodegradable at high concentrations, representing a serious  
49 health and environmental hazard (Cheng et al, 2020). It can cause respiratory, digestive and  
50 mental disorders, skin irritation, and conditions such as methemoglobinemia, tissue necrosis,  
51 jaundice and cardiac disorders, leading to serious or even fatal effects (Mashkoo et Nasar  
52 2020, Khan et al. 2022). This highlights the urgent need to identify and implement effective  
53 solutions for treating wastewater containing these harmful dyes to mitigate their adverse  
54 environmental and health impacts. Methylene blue, one of the most commonly used and  
55 studied dyes, presents significant challenges to conventional degradation technologies. While  
56 biological wastewater treatment is considered environmentally friendly and cost-effective, it  
57 is often ineffective for treating dye effluents due to the complex and poorly biodegradable nature  
58 of dyes (Bedin et al. 2016, Allouche et al. 2017, Jalal et al. 2024, Kamati et al. 2024, Kumar  
59 et al. 2017, Periyasamy et al. 2024) . Adsorption is another widely used method due to its  
60 simplicity, relatively low cost, and effectiveness in reducing toxicity (Liu et al. 2016, Nassar  
61 et al. 2016). However, this technology has the disadvantage of generating secondary pollution  
62 that is potentially dangerous for the environment and human health (Kumar et al. 2017).

63  
64 Today, Advanced Oxidation Processes (AOPs) represent a promising alternative based on  
65 the generation of highly reactive oxidant species that can effectively degrade all kinds of  
66 organic compounds (Ling et al. 2016, Wen et al. 2019). These technologies are used to  
67 remove toxic organic compounds such as MB (Zhang et al. 2019<sup>a</sup>, Khan et al. 2022).  
68 Photocatalytic degradation is one of the AOPs commonly used for dye degradation (Chih-Chi  
69 et al. 2018, Venkatraman et al. 2020, Deepika et al. 2023). In this process, a semiconductor  
70 used as a photocatalyst absorbs light and uses the photon energy to contribute significantly  
71 to the degradation of organic compounds (Shen et al. 2017, Wu et al. 2023). However, the  
72 photocatalytic activity of the semiconductor depends on its band gap and its ability to generate  
73 electron-hole pairs that give rise to free radicals that undergo secondary reactions (Zhang et  
74 al. 2019<sup>b</sup>). According to the literature, the semiconductors ZnO, CdS, TiO<sub>2</sub>, and their  
75 composites are widely used for the photocatalytic degradation of dyes, especially methylene  
76 blue (Enéderson et al. 2010, Ranfang et al. 2014, Velanganni et al. 2018, Dinda et al. 2023).  
77 In the case of direct photolysis, the energy from the light is absorbed directly by the organic  
78 compound, resulting in its molecular decomposition (Bendjama et al. 2019). **The main  
79 drawback of this method is that it requires an extended degradation period and often results  
80 in the transformation of the parent compound, sometimes generating more toxic intermediates**

(Aziz et al. 2020). However, it appears that the direct photolysis of MB alone is insufficient to significantly degrade it under UV light irradiation (Rashad et al. 2016). Indeed, the literature reports that the degradation rate of MB after 10h under solar irradiation was 7.9 % (Siong et al. 2019). But, using the UV/H<sub>2</sub>O<sub>2</sub> system for the degradation of organic compounds allows very high degradation rates to be achieved compared to simple UV irradiation (Dong et al. 2021). Photolysis in the presence of H<sub>2</sub>O<sub>2</sub> can lead to mineralisation of organic compounds (Ae-Jung et al. 2022). However, the effectiveness of this process is heavily reliant on the concentration of H<sub>2</sub>O<sub>2</sub>. Using an excessive concentration of H<sub>2</sub>O<sub>2</sub> can inhibit the process by consuming hydroxyl radicals (Bingliang et al. 2022, Ghosh et al. 2024). Also, the degradation of compounds by UV/NO<sub>3</sub><sup>-</sup> and UV/Cl<sup>-</sup> processes has been reported in the literature (Wang et al. 2017, Sicheng et al. 2022, Zhiquan et al. 2022). However, work on the degradation of compounds employing the UV/I<sup>-</sup> or UV/I<sup>-</sup>+NaCl system is still in its infancy to the best of our knowledge.

The purpose of the present work was: (1) evaluate the influence of different parameters on the UV photolysis of MB, such as the concentration of MB, I<sup>-</sup>, NaCl, pH and the amount of H<sub>2</sub>O<sub>2</sub>; (2) explore the synergistic effect of I<sup>-</sup> and NaCl, and H<sub>2</sub>O<sub>2</sub> and NaCl on MB photolysis degradation. We hope that this work will be useful for future research in this field.

## 2. MATERIAL AND METHODS

### 2.1. Reagents

Methylene blue (Purity >98.0) was obtained from Aladdin Chemicals Co. Ltd. (Shanghai, China). Hydrogen peroxide (H<sub>2</sub>O<sub>2</sub>) was produced by SCHARLAU. Sodium chloride (NaCl) and sodium iodide (I<sup>-</sup>) were manufactured by Merck. The solid products and reagents are stored at the ambient temperature and protected from light. The pH of the electrolyte was adjusted using sodium hydroxide (Prolabo) and Sulfuric acid (Fluka), and pH solution was recorded with Banté pH meter using a combination pH electrode. The calibration of the electrode was performed using buffer solutions of pH 4.0, 7.0 and 9.0. Solutions were prepared with distilled water. All the experiments were performed at laboratory temperature.

### 2.2. Experimental procedure

The photolysis measurements were performed with a Suntest sun simulator (ORIGINAL HANAU) (Fig. 1), equipped with a 1500 W xenon lamp disposed horizontally. A 100 mL of MB solution, prepared in distilled water, was introduced into the solar simulator. The first sample (2 mL) is collected at t=0, then the solar simulator is switched on and the chronometer is started. Samples of approximately 2 mL are taken, without any filtration, at different well-defined times, and their absorbance at 665 nm was recorded using a HACH DR 6000 UV-vis spectrophotometer. The concentration of MB degraded during photolysis was quantified via a calibration curve obtained by measuring the absorbance of MB solutions with known concentrations (0, 1, 3, 6, 9, 12 mg/L).

The calibration curve obtained is represented by a straight line described by the equation 1:

$$\text{Absorbance} = 0.2304 C + 0.081, \quad R^2 = 0.9901 \quad (1)$$

Then, the percentages of degradation in the absence and presence of oxidants were calculated using the equation 2:

$$\% \text{Degradation} = \frac{c_0 - c_t}{c_0} \times 100 \quad (2)$$

131 Where  $C_0$  is the initial concentration of MB, while  $C_t$ , denotes its concentration after irradiation  
132 for a time  $t$ .

133

134 Experimental conditions, including the initial MB concentration, pH, NaI, NaCl,  $H_2O_2$ ,  
135 NaI+NaCl and NaCl+ $H_2O_2$  were adjusted as needed to explore their influence on the MB  
136 photolysis. The kinetics of MB photodegradation were determined by fitting the experimental  
137 data to a pseudo- first-order kinetic model (Equation 3) (Wang et al. 2021). The obtained  $R^2$   
138 values indicated that the degradation process in this study followed a pseudo-first-order kinetic  
139 model. The plot of  $\ln(C_t/C_0)$  as a function of time ( $t$ ) was used to determine  $K_{obs}$ , the values of  
140 which are shown for each parameter in Table 1.

141

$$142 \quad \ln\left(\frac{C_t}{C_0}\right) = -k_{obs}t \quad (3)$$

143

144 Where  $C_0$  and  $C_t$  are the initial and different time concentrations of the MB, respectively.  $k_{obs}$   
145 represents the first-pseudo-order constant.

146

147

148

149

150

151

152

153

154

155

156

157

158

159



Fig.1. Experimental setup used for photodegradation of MB

160

## 161 3. RESULTS AND DISCUSSION

162

163

163

164

165

166

167

168

169

170

171

172

173

174

175

176

177

178

179

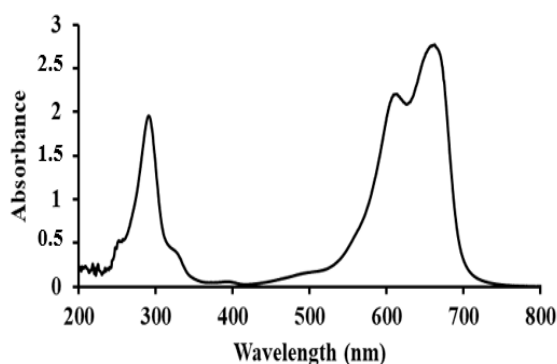
180

181

### 3.1 MB UV-Vis absorption spectrum

The colour of MB depends on its chromophoric and auxochromic groups. The chromophore group is the part of the molecule responsible for absorbing light (Khan et al. 2022). In the case of MB compound, the N-S conjugated system on the central aromatic heterocycle is the main chromophore, allowing it to absorb specific wavelengths, contributing to its blue colour. The auxochrome group does not absorb light directly, but modifies the chromophore's absorption. It influences the absorption wavelength and can also affect the intensity and stability of the colour. In MB, amine groups (-NH) and other substituents can act as auxochromes, enhancing the effect of the chromophore.

The UV-Vis absorption spectrum of BM in solution, presented in Fig.2, exhibits a localized intense peak at 665 nm attributed to the monomer form of the MB, and a shoulder peak at 610 nm associated with a dimer form of the dye studied (Wang et al. 2021). Indeed, the peak at 665 nm will be the peak that will allow us to follow the concentration of methylene blue. Furthermore, the 295 nm peak is associated with substituted benzene rings.



182  
183  
184  
185  
186  
187  
188  
189  
190  
191  
192  
193

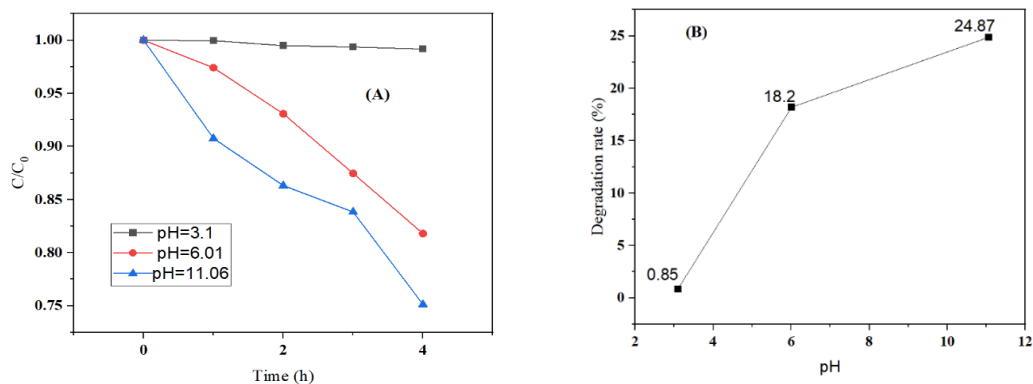
**Fig.2. UV-visible absorption spectrum of methylene blue at pH=6.01**

**3.2. Initial pH Effect**

194 The effect of pH on the direct MB photolysis was performed at different pH values (3.1; 6.8  
195 and 11.06) for 10 mg/L of MB solution with a volume of 100 mL during 04 hours of treatment.  
196 Figure 3 (A) exhibits a difference in the reactivity of MB as a function of the initial pH of the  
197 medium. The rate of degradation was rapid at pH 11.06 compared to pH 6.01 and pH 3.1. The  
198 removals obtained increased from 0.85 to 24.87%, and the  $k_{obs}$  increased from 0.017 to 0.065  
199 when pH increased from 3 to 11.06 showing the enhancement of MB degradation with  
200 increasing pH. As pH 3.1 is lower than  $pK_a$  3.8 (Khan et al. 2022), MB is mainly in protonated  
201 form, which could limit its interaction with photons emitted by light. At pH 6.01, degradation is  
202 significantly improved because the compound is no longer in the protonated form and  
203 therefore reacts more readily with light than at pH 3.1. At alkaline pH, the degradation  
204 percentage reaches its maximum (24.87%). **The fact can explain this at this pH, MB is  
205 deprotonated, which increases its reactivity with free radicals, leading to a higher degradation  
206 rate.** Furthermore, alkaline conditions can promote the formation of hydroxyl radicals, which  
207 are powerful oxidants, thereby improving MB degradation.  $OH^\bullet$  radicals will in turn react with  
208 each other to form peroxide ( $H_2O_2$ ) which plays a prominent role in the degradation process  
209 (equations 4-6) (Khan et al. 2022).



213  
214  
215  
216  
217  
218  
219  
220  
221  
222

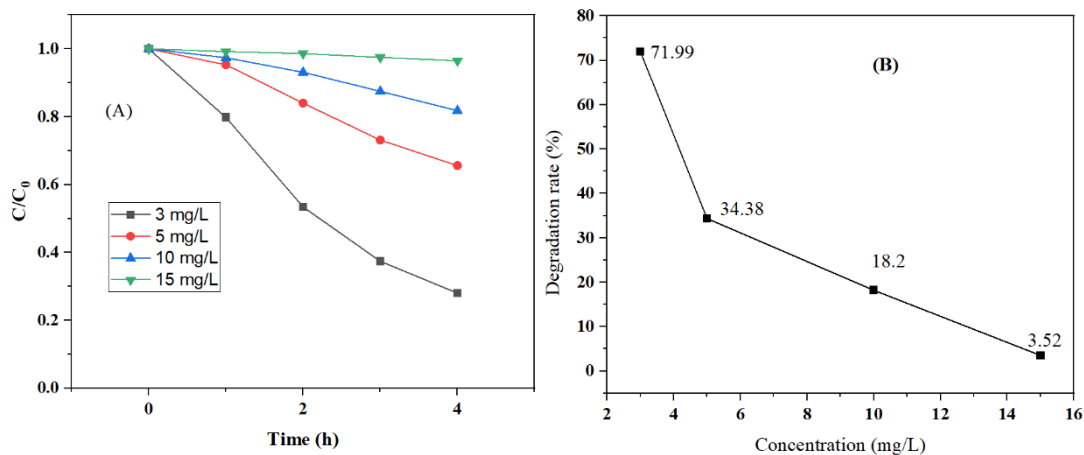


223 **Fig.3. (A) Effect of pH on MB degradation versus time; (B) MB concentration reduction**  
224 **rate for different pH over a period of 4 hours; [MB] = 10 mg/L.**  
225

226 **3.3. Effect of MB concentration**

227 The effect of MB initial concentration was investigated in the range of 3 to 15 mg/L at  
228 unadjusted pH of 6.01 during 4 hours of UV-C irradiation. The results obtained, shown in **Fig.4**

229 (A), revealed a decreasing of the degradation rate of MB when increasing the initial  
 230 concentration. The concentration removal determined after 4 hours of UV-C irradiation are  
 231 71.99, 34.38, 18.2 and 3.52 %, respectively, for 3, 5, 10 and 15 mg/L (Fig.4 (B)). The  $K_{obs}$   
 232 values decreased also from 0.33 to 0.009  $h^{-1}$  when MB concentration increased from 3 to 15  
 233 mg/L (Table 1). It appears that increasing the initial concentration has an inhibitory effect of  
 234 the performance of photolysis. This can be attributed to the formation of more oxidation  
 235 products as the concentration of MB increases during the photolysis process, which may act  
 236 as scavengers for reactive radicals. Furthermore, the addition of excess MB could enhance  
 237 an internal filtering effect, so that the penetration of photons entering the solution would be  
 238 significantly reduced, leading to an apparent decrease in the proportion of the incident UV flux  
 239 absorbed by MB molecule (Wang et al. 2021).



252  
 253  
 254 **Fig.4. (A) Effect of MB concentration on degradation versus time; (B) MB**  
 255 **concentration reduction rate for different initial MB concentrations after 4 hours; pH =**  
 256 **6.01.**

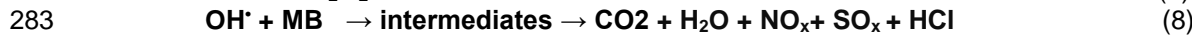
### 257 3.4. Effect of H<sub>2</sub>O<sub>2</sub>

259 Photolysis reactions involve the generation of highly active OH<sup>•</sup> radicals. The radicals formed  
 260 during direct photolysis are considered to be oxidants for various chemicals. For this purpose,  
 261 hydrogen peroxide's influence on MB degradation during the photolysis process was  
 262 investigated in a solution containing 10 mg/L of MB for 4 h of irradiation. The degradation of  
 263 MB at pH 6.01 (unadjusted) was followed as a function of irradiation time for different amounts  
 264 of H<sub>2</sub>O<sub>2</sub> within the range between 0 and 1 mL.  
 265

266 **Fig.5** depicts the degradation efficiency of MB solution as a function of the volume of H<sub>2</sub>O<sub>2</sub>  
 267 added to the solution. H<sub>2</sub>O<sub>2</sub> had a strong positive effect on the degradation of MB. The  
 268 percentage of MB degradation are 88.82 and 92 % by adding 0.5 and 1 mL of H<sub>2</sub>O<sub>2</sub>,  
 269 respectively, which surpassed that obtained without hydrogen peroxide (18.2 %) by 4.88 and  
 270 5.05 times, respectively. This means that H<sub>2</sub>O<sub>2</sub> significantly promotes the photolysis of MB  
 271 degradation under the conditions we work in, which is consistent with the literature (Wenhui  
 272 et al. 2019). This behavior is attributed to the significant quantity of the powerful and  
 273 unselective radicals (OH<sup>•</sup>) produced in the UV/H<sub>2</sub>O<sub>2</sub> (Equation 7). These radicals attack the  
 274 molecule and produce the molecule radicals, MB<sup>•</sup> in our case (Equation 8) (Ali et al. 2024,  
 275 Hanadi et al. 2021). These MB radicals undergo further oxidation and are converted into  
 276 reaction intermediates that can lead to CO<sub>2</sub>, H<sub>2</sub>O, NO<sub>x</sub>, SO<sub>x</sub>, and HCl as described by Ali and  
 277 collaborators (equation 8) (Ali et al. 2024). In fact, the intermediates products of MB included  
 278 2-amino-5-(N-methyl formamide)benzene sulfonic acid (m/z =230), 2-amino-5-(methyl

279 amino)-hydroxybenzene sulfonic acid ( $m/z = 218$ ), benzenesulfonic acid ( $m/z = 158$ ), phenol  
 280 ( $m/z = 94$ ) and other, according to Ali et al. (2024) and Yang et al. (2017).

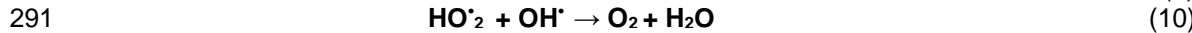
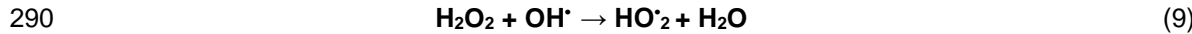
281



284

285 However, we note a slight increase of the MB degradation percentage when the amount of  
 286  $\text{H}_2\text{O}_2$  passed from 0.5 to 1 mL, which means a higher amount of  $\text{H}_2\text{O}_2$  may result in a reduction  
 287 of the UV/ $\text{H}_2\text{O}$  process efficacy due to the generation of  $\text{HO}_2^\bullet$  and  $\text{O}_2$  instead of  $\text{OH}^\bullet$  (Equations  
 288 9-10), which are less powerful than hydroxyl radicals.

289



292

293

294

295

296

297

298

299

300

301

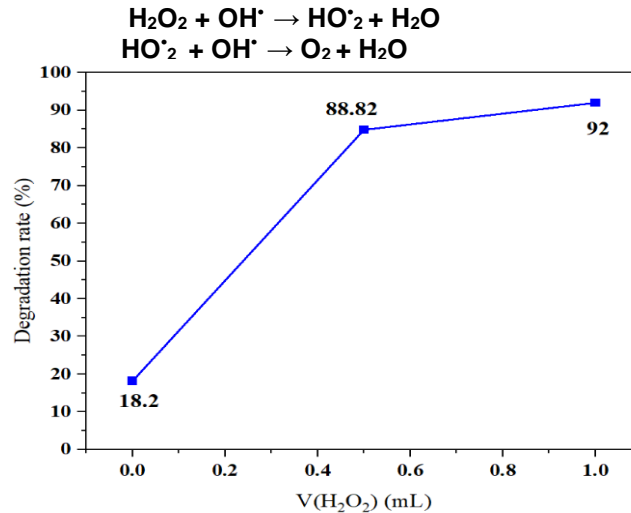
302

303

304

305

306



307

307 **Fig.5. MB concentration removal for different  $\text{H}_2\text{O}_2$  volume over a period of 4 hours;**

308 **[MB] = 10 mg/L; pH = 6.01.**

309

310

311

312

313

314

315

316

317

318

319

320

321

322

323

324

325

326

327

328

329

330

330

### 3.5. Effect of NaI

The effect of sodium iodide (NaI) on the photolysis degradation of 10 mg/L of methylene blue solution was conducted at an unadjusted pH of 6.01 over 4 hours of treatment. Different NaI concentrations (0.075 and 0.01 M) were used to evaluate the MB degradation kinetics. As shown in Fig.6(A), iodide ions contributed to the degradation of MB. After 4 hours, degradation percentages of 77.48% and 83.77% were achieved for 0.0075 M and 0.01 M NaI, respectively. These values are 4.26 and 4.60 times greater than the 18.2% obtained from photolysis of MB only (without NaI). The determined Kobs values were 0.708 h<sup>-1</sup> and 0.854 h<sup>-1</sup> for 0.0075 M and 0.01 M NaI, respectively, both higher than those observed in photolysis without NaI. These results suggested a strong participation of the reactive of intermediates species from I<sup>-</sup> in the degradation of MB. I<sup>-</sup> might absorb photons leading to its dissociation into I<sup>•</sup> which then react with methylene blue, leading to degradation reactions (Equation 11) (Tang et al. 2021, Xu et al. 2024). Furthermore, iodide radicals can combine to form I<sub>2</sub>, which can subsequently react with I<sup>-</sup> to form I<sub>3</sub><sup>-</sup> (Equations 12-13) (Kalmár et al. 2014, Tang et al. 2021, Xu et al. 2024). In a further step, I<sup>•</sup> can react with I<sup>-</sup> to form I<sub>2</sub><sup>•-</sup>, the latter being less potent than I<sup>•</sup> (Grebel et al. 2010, Kalmár et al. 2014) (Equation 14).



331



(14)

332 The evolution of methylene blue concentration in the presence of NaI was compared to that  
 333 in the presence of H<sub>2</sub>O<sub>2</sub> (Fig.5(B)). This figure shows that photolysis has a different effect on  
 334 the degradation of Methylene Blue depending on whether it takes place in the presence of NaI  
 335 or H<sub>2</sub>O<sub>2</sub>. In the presence of NaI, the concentration of the parent compound decreases rapidly  
 336 during the first two hours of treatment and then stabilises almost completely. In contrast, in  
 337 the presence of H<sub>2</sub>O<sub>2</sub>, the initial concentration continues to decrease progressively throughout  
 338 the degradation process. These results reflect the different degradation mechanisms of  
 339 methylene blue depending on the reagents used. In the presence of NaI, the reaction is  
 340 dominated by oxidative species of iodine, which favours a rapid initial attack of methylene  
 341 blue, but is limited in time by the probable depletion of the concentration of the active agent.  
 342 Conversely, with H<sub>2</sub>O<sub>2</sub>, photolysis continuously generates hydroxyl radicals, ensuring  
 343 progressive and sustained degradation of the BM throughout the process.  
 344

345

346

347

348

349

350

351

352

353

354

355

356

357

358

359

360

361

362

363

364

365

366

367

368

369

370

371

372

373

374

375

376

377

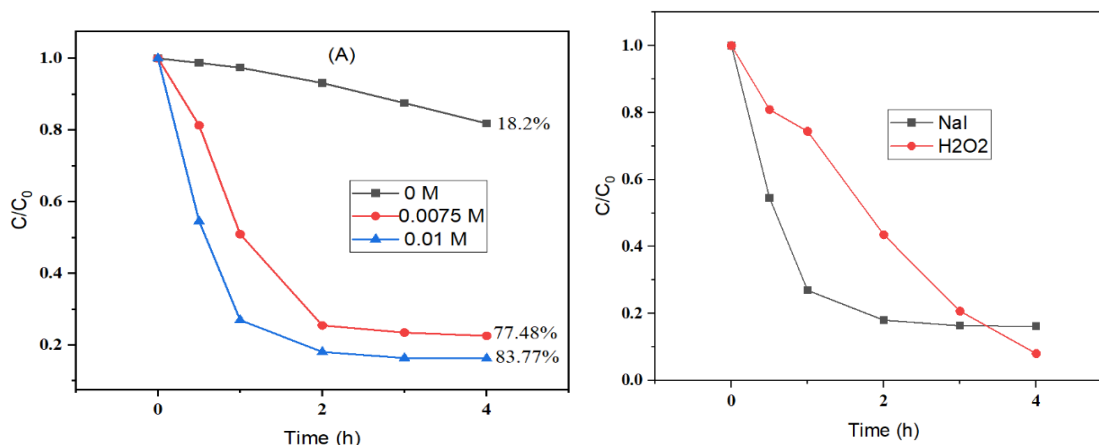
378

379

380

381

382



359 **Fig.6. (A) Evolution of MB concentration (10 mg/L) over time for different NaI**  
 360 **concentrations and (B) Comparison of C<sub>MB</sub> evolution in the presence of NaI and H<sub>2</sub>O<sub>2</sub>**

361

362

### 362 3.6. Effect of NaCl and NaCl combined with H<sub>2</sub>O<sub>2</sub> or NaI

363

364

365

366

367

368

369

364 Cl<sup>-</sup> ions are commonly found in water bodies (Luo et al. 2020), and can influence the pollutant  
 365 removal processes. **Fig.7(A)** displays the influence of Cl<sup>-</sup> ions on the photolysis of MB. The  
 366 investigations were performed in 10 mg/L of MB solution at unadjusted pH. Cl<sup>-</sup> had an inhibitory  
 367 effect on the photodegradation of MB and the removal efficiency decreased from 18.2 %  
 368 (absence of Cl<sup>-</sup>) to 6.2% (presence of Cl<sup>-</sup>).

370

371

372

373

374

375

376

377

378

379

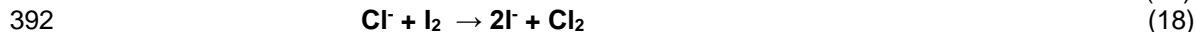
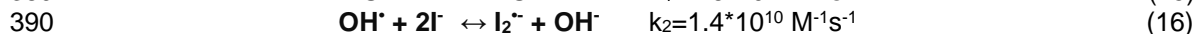
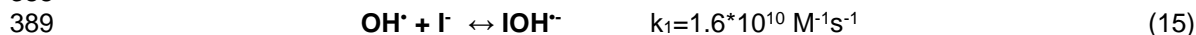
380

381

382

370 The inhibitory effect of chloride ions can be explained by their reaction with hydroxyl radicals  
 371 which could lead to the generation of other less reactive inorganic radical species (Cl<sup>•</sup>, Cl<sub>2</sub><sup>•</sup>  
 372 and HOCl<sup>•</sup>) (Lu et al. 2005, Hilla et al. 2007, Kambiré et al. 2022). Chloride ions can also  
 373 influence the optical properties of the solution, affecting the way light is absorbed and,  
 374 consequently, the efficiency of photolysis of MB. Cl<sup>-</sup> ions have been recognized as inhibitors,  
 375 along with other inorganic ions such as SO<sub>4</sub><sup>2-</sup>, NO<sub>3</sub><sup>-</sup>, HCO<sub>3</sub><sup>-</sup>, and H<sub>2</sub>PO<sub>4</sub>/HPO<sub>4</sub><sup>2-</sup> ions, for the  
 376 degradation of organic compounds by photolysis (Hilla et al. 2007, Wen et al. 2019).  
 377 Experiments were conducted by adding, to 10 mg/L MB + 0.01 M NaCl, 1 mL H<sub>2</sub>O<sub>2</sub> and 0.01  
 378 M NaI separately to the mixture. According to the results obtained (**Fig.7 (B)**), it's evident that  
 379 the presence of H<sub>2</sub>O<sub>2</sub> or NaI significantly improves the removal of MB during photolysis  
 380 treatment. After 4 h of treatment, the rates obtained were 84.9 % and 88.1 % in the presence  
 381 of H<sub>2</sub>O<sub>2</sub> and NaI, respectively. The coexisting I<sup>-</sup> and Cl<sup>-</sup> synergistically affect the removal of MB  
 382 in the UV/Cl<sup>-</sup>-I<sup>-</sup> system compared to when NaI (83.77 %) and NaCl (6.2 %) were present alone

383 in the reaction medium. This improvement could be explained by the fact that hydroxyl radicals  
 384 react more rapidly with iodide ions to form the reactive intermediates species (RIS) of iodine  
 385 compared with chloride ions, which can contribute to the degradation of MB (Equations 15-  
 386 17). Furthermore, as iodine is photosensitive, I<sub>2</sub> could be formed in the reaction medium and  
 387 react with chloride ions to form Cl<sub>2</sub> (equation 18), which is a powerful oxidant.



393

394 However, when NaCl and H<sub>2</sub>O<sub>2</sub> are simultaneously present in the medium, a slight decrease  
 395 in the efficiency of MB degradation was observed compared to the case where H<sub>2</sub>O<sub>2</sub> (92 %)  
 396 alone was present in the medium. This finding is consistent with the works of Muruganandham  
 397 (Muruganandham and Swaminathanm 2004) who demonstrated that the presence of chloride  
 398 ions resulted in a slight decrease in the degradation rate of reagent orange 4 by UV/H<sub>2</sub>O<sub>2</sub>.  
 399 According to these findings, the combination of NaCl and NaI (UV/Cl<sup>-</sup>-I<sup>-</sup> system) exhibits the  
 400 best performance for the photodegradation of methylene blue (MB). It achieves 88.1% removal  
 401 efficiency after 4 hours.

402

403

404

405

406

407

408

409

410

411

412

413

414

415

416

417

418

419

420

421

422

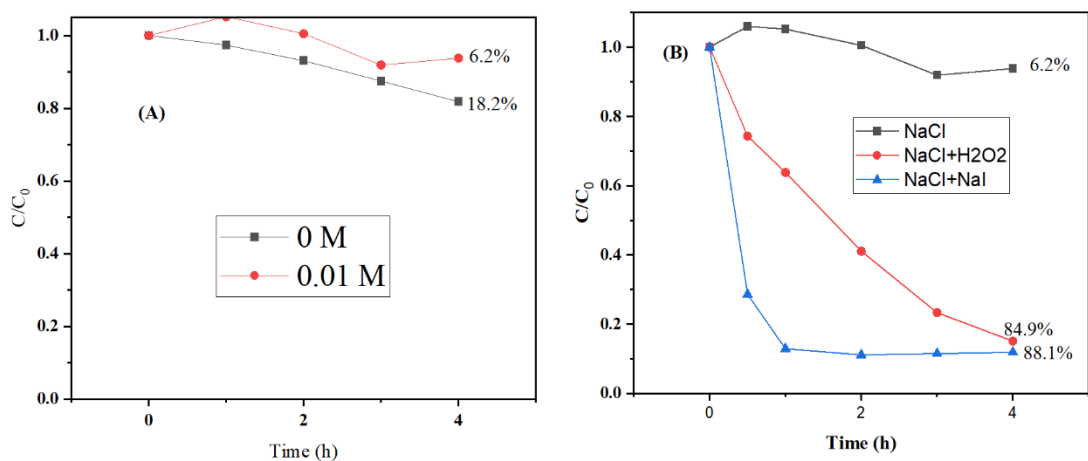


Fig.6. (A) Evolution of MB concentration (10 mg/L) over time in the presence of 0.005 M NaCl, (B) Effect of NaCl+ H<sub>2</sub>O<sub>2</sub> (1 mL) and NaCl+NaI (0.01 M) combination

Table 1. Pseudo-first order rate describing MB oxidation in various conditions

Parameters	MB concentration (mg/L)				Initial pH		H <sub>2</sub> O <sub>2</sub> (mL)		NaI (M)		NaCl (M)	
	3	5	10	15	3.1	6.01	11.06	0.5	1	0.0075	0.01	0.01
k <sub>obs</sub> (h <sup>-1</sup> )	0.33	0.111	0.051	0.009	0.017	0.051	0.065	0.488	0.62	0.708	0.854	-
R <sup>2</sup>			0.974	0.986	0.977			0.961	0.994	0.964		

423

#### 424 4. CONCLUSION

425 Photolysis under artificial solar irradiation was employed to degrade the widely used model  
426 dye methylene blue (MB). The initial concentration of MB significantly influences the  
427 degradation efficiency, with lower concentrations leading to better performance in the process.  
428 A basic medium favors the photolytic degradation of MB, as it enhances the production of  
429 hydroxyl radicals through hydroxide ions. Additionally, hydrogen peroxide plays a crucial role  
430 in accelerating the photolytic degradation of MB. The presence of iodide ions (I<sup>-</sup>) notably  
431 improves the degradation kinetics reducing the experiment time, while the effect of sodium  
432 chloride (NaCl) is less significant, resulting in slower degradation. However, when combined  
433 with hydrogen peroxide or iodide, the degradation rate of MB is significantly enhanced. The  
434 experiments conducted were analyzed using the pseudo-first-order kinetic model, suggesting  
435 that the degradation process follows this kinetic behavior under various conditions. In  
436 conclusion, the photolytic degradation of MB, especially in the presence of hydrogen peroxide,  
437 iodide ions, or combinations of these, demonstrates an effective oxidation process for breaking  
438 down the organic dye.

439

#### 440 ACKNOWLEDGEMENTS

441

442 The authors state that they have not received any explicit funding for this work.

#### 443 COMPETING INTERESTS

444

445 The authors declare no conflicts of interest regarding the publication of this paper.

446

#### 447 AUTHORS' CONTRIBUTIONS

448

449 **Foffié Thiery Auguste Appia** conceived the work, participated in the critical revision of the  
450 article, **Tiémélé Ghislaine Désirée Kouassi** and **Charlène Sandra Coulibaly** carried out the  
451 data collection, **Kouakou Jocelin Kimou** wrote the first draft, **Jean-Claude Meledje**  
452 participated in the critical revision of the article and **Lassiné Ouattara** supervised the work.

453 All authors read and approved the final manuscript.

454

#### 455 REFERENCES

456

457 Abd-Elhamid, A.I., Emran, M., El-Sadek, M.H., El-Shanshory, A.A., Soliman, H.M.A., Akl, M.A.  
458 et al. (2020). Enhanced removal of cationic dye by eco-friendly activated biochar derived from  
459 rice straw. *Applied Water Science*, 10 (1), 1-11. <https://doi.org/10.1007/s13201-019-1128-0>

460

461 Ae-Jung, H., Jaewon, L., Youngho, & C., Zoh, K.-D. (2022). Propiconazole degradation and  
462 its toxicity removal during UV/H<sub>2</sub>O<sub>2</sub> and UV photolysis processes. *Chemosphere*, 302,  
463 134876. <https://doi.org/10.1016/j.chemosphere.2022.134876>

464

465 Ali, M.A., Maafa I.M., & Qudsieh, I.Y. (2024). Photodegradation of Methylene Blue Using a  
466 UV/H<sub>2</sub>O<sub>2</sub> Irradiation System. *Water*, 16, 453. <https://doi.org/10.3390/w16030453>

467

468 Allouche, F.N., & Yassaa, N. (2017). Potential adsorption of methylene blue from aqueous  
469 solution using green macroalgae *Posidonia oceanica*. IOP Conference Series: Materials  
470 Science and Engineering. 323, 012006. <https://doi.org/10.1088/1757-899X/323/1/012006>  
471

472 **Atta, D., Wahab, H.A., Ibrahim, M.A., Battisha, & I.K. (2024). Photocatalytic degradation of**  
473 **methylene blue dye by ZnO nanoparticle thin films, using Sol-gel technique and UV laser**  
474 **irradiation. Scientific reports, 14, 26961. <https://doi.org/10.1038/s41598-024-76938-1>**  
475

476 Aziz, A., Ali, N., Khan, A., Bilal, M., Malik, S., Ali, N., et al. (2020). Chitosan-zinc sulfide  
477 nanoparticles, characterization and their photocatalytic degradation efficiency for azo dyes.  
478 International Journal of Biological Macromolecules, 153, 502–512.  
479 <https://doi.org/10.1016/j.ijbiomac.2020.02.310>  
480

481 Bedin, K.C., Martins, A.C., Cazetta, A.L., Pezoti, O., & Almeida, V.C. (2016). KOH-activated  
482 carbon prepared from sucrose spherical carbon: Adsorption equilibrium, kinetic and  
483 thermodynamic studies for Methylene Blue removal. Chemical Engineering Journal, 286, 476–  
484 484. <https://doi.org/10.1016/j.cej.2015.10.099>  
485

486 Bendjama, H., Merouani, S., Hamdaoui, O., & Bouhelassa, M. (2019). UV-photolysis of  
487 Chlorazol Black in aqueous media: Process intensification using acetone and evidence of  
488 methyl radical implication in the degradation process. Journal of Photochemistry &  
489 Photobiology A: Chemistry, 368, 268–275. <https://doi.org/10.1016/j.jphotochem.2018.09.047>  
490

491 Benkhaya, S., M'rabet, S., & El Harfi, A. (2020). A review on classifications, recent synthesis  
492 and applications of textile dyes. Inorganic Chemistry Communications, 115, 107891.  
493 <https://doi.org/10.1016/j.inoche.2020.107891>  
494

495 Bingliang, Z., Zhuoyao, F., Shu, W., Xifeng, S., Guo, B., Jie, G., et al. (2022). Effect of  
496 bromide on molecular transformation of dissolved effluent organic matter during ozonation,  
497 UV/H<sub>2</sub>O<sub>2</sub>, UV/persulfate, and UV/chlorine treatments. Science of The Total Environment, 811,  
498 152328. <https://doi.org/10.1016/j.scitotenv.2021.152328>  
499

500 **Cheng, J., Zhan, C., Wu, J., Cui, Z., Si, J., Wang, Q., Peng, X., & Turng, L.S. (2020). Highly**  
501 **Efficient Removal of Methylene Blue Dye from an Aqueous Solution Using Cellulose Acetate**  
502 **Nanofibrous Membranes Modified by Polydopamine. ACS Omega, 5, 5389–5400.**  
503 <https://doi.org/10.1021/acsomega.9b04425>  
504

505

506 Chih-Chi, Y., Ruey-An, D., Ku-Fan, C., Giin-Shan, C., & Tsai, Y.-P. (2018). The photocatalytic  
507 degradation of methylene blue by green semiconductor films that is induced by irradiation by  
508 a light-emitting diode and visible light. Journal of the Air & Waste Management Association,  
509 68:1, 29-38. <https://doi.org/10.1080/10962247.2017.1358222>  
510

511 Contreras, M., Grande-Tovar, C.D., Vallejo, W., & Chaves-López, C. (2019). Bio-Removal of  
512 Methylene Blue from Aqueous Solution by *Galactomyces geotrichum* KL20A. Water. 11, 282.  
513 <https://doi.org/10.3390/w11020282>  
514

515 Deepika, C., Dinesh, K., Preeti T., & Atul, T. (2023). Visible light induced photocatalytic  
516 degradation of methylene blue dye by using Mg doped Co-Zn nanoferrites. Materials Research  
517 Bulletin, 162, 112205. <https://doi.org/10.1016/j.materresbull.2023.112205>  
518

519 Dinda, G.A., Saharman, G., Andriyani, D.J.T., Averroes, F.R.P., Mahyuni, H., Zhihao, Y., et  
520 al. (2023). Photocatalytic Degradation of Methylene Blue Using N-Doped ZnO/Carbon Dot (N-

521 ZnO/CD) Nanocomposites Derived from Organic Soybean. ACS Omega, 8, 17, 14965–14984.  
522 <https://doi.org/10.1021/acsomega.2c07546>  
523

524 Dong, W., Yang, C., Zhang, L., Su, Q., Zou, X., Xu, W. et al. (2018). Highly efficient UV/H<sub>2</sub>O<sub>2</sub>  
525 technology for the removal of nifedipine antibiotics: Kinetics, co-existing anions and  
526 degradation pathways. PLoS One, 16 (10), e0258483.  
527 <https://doi.org/10.1371/journal.pone.0258483>  
528

529

530 Enéderson, R., Diego, I.P., João, H.Z.D.S., Sibeles, B.C.P., & Fábio, G.P. (2010). Bentonites  
531 impregnated with TiO<sub>2</sub> for photodegradation of methylene blue. Applied Clay Science, 48 (4)  
532 602–606. <https://doi.org/10.1016/j.clay.2010.03.010>  
533

534 Grebel, J.E., Pignatello, J.J., & Mitch, W.A. (2010). Effect of halide ions and carbonates on  
535 organic contaminant degradation by hydroxyl radical-based advanced oxidation processes in  
536 saline waters, Environmental Science & Technology, 44 (17), 6822–6828.  
537 <https://doi.org/10.1021/es1010225>  
538

539 Ghosh, A., Asce A.A.A.M., Mondal, B., Barbhuiya N.H., & Das, I. (2024). Efficacious  
540 Degradation of 2,4-Dichlorophenoxyacetic Acid by UV–H<sub>2</sub>O<sub>2</sub> Advanced Oxidation and  
541 Optimization of Process Parameters Using Response Surface Methodology. Journal of  
542 Hazardous, Toxic, and Radioactive Waste, 28 (3). <https://doi.org/10.1061/JHTRBP.HZENG-13>  
543  
544

545 Jalal U., Muhammad I., Humam A., Saima B., Tanzeel U.R., Shahzil M., et al. (2024).  
546 Biodegradation and decolorization of methylene blue, reactive Black-5, and toluidine blue-O  
547 from an aqueous solution using the polyphenol oxidase enzyme. Frontiers in Sustainable Food  
548 Systems, 7, 1320855. <https://doi.org/10.3389/fsufs.2023.1320855>  
549

550 Kalmár, J., Dóka, É., Lente, G., & Fábián, I. (2014). Aqueous photochemical reactions of  
551 chloride, bromide, and iodide ions in a diode-array spectrophotometer. Autoinhibition in the  
552 photolysis of iodide ions. Dalton Transactions, 43, 4862. <https://doi.org/10.1039/c3dt53255k>  
553

554 Kambiré, O., Abollé, A., Kouakou, A.R, Koffi, A.E., Koffi, K. S., Kouadio, K. Etienne., et al.  
555 (2022). Photocatalytic degradation of methyl orange in an aqueous solution in presence of  
556 copper oxide. Journal de la Société Ouest-Africaine de Chimie, 051, 45 – 55  
557

558 Khan, I, Saeed, K., Zekker, I., Zhang, B., Hendi, A.H., Ahmad, A., et al. Review on Methylene  
559 Blue: Its Properties, Uses, Toxicity and Photodegradation. Water, 14 (2), 242.  
560 <https://doi.org/10.3390/w14020242>  
561

562 Kumar, M.S., Sonawane, S.H., & Pandit, A.B. (2017). Degradation of methylene blue dye in  
563 aqueous solution using hydrodynamic cavitation based hybrid advanced oxidation processes.  
564 Chemical Engineering and Processing: Process Intensification, 2017,122, 288-295.  
565 <https://doi.org/10.1016/j.cep.2017.09.009>  
566

567 Ling, L., Sun, J., Fang, J., & Shang, C. (2016) Kinetics and mechanisms of degradation of  
568 chloroacetonitriles by the UV/H<sub>2</sub>O<sub>2</sub> process. Water research, 99, 209-215.  
569

570 Liu, J., Li, E., You, X., Hu, C., & Huang, Q. (2016). Adsorption of methylene blue on an agro-  
571 waste oiltea shell with and without fungal treatment. Scientific reports, 6, 38450.  
572 <https://doi.org/10.1038/srep38450>  
573

574 Lu, M.-C., Chang, Y.-F., Chen, I.-M., & Huang, Y.-Y. (2005). Effect of chloride ions on the  
575 oxidation of aniline by Fenton's reagent. *Journal of Environmental Management*, 75, 177–182.  
576 <https://doi.org/10.1016/j.jenvman.2004.12.003>  
577

578 Luo, C., Wu, D., Gan, L., Cheng, X., Ma, Q., Tan, D., et al. (2020). Oxidation of Congo red by  
579 thermally activated persulfate process: Kinetics and transformation pathway. *Separation and*  
580 *Purification Technology*, 244, 116839. <https://doi.org/10.1016/j.seppur.2020.116839>  
581

582 **Mashkoo F, & Nasar A. (2020). Magsorbents: Potential candidates in wastewater treatment**  
583 **technology–A review on the removal of methylene blue dye. *Journal of magnetism and***  
584 **magnetic materials, 500, 166408. : <https://doi.org/10.1016/j.jmmm.2020.166408>**  
585  
586

587 Muruganandham, M., & Swaminathanm, M. (2004). Photochemical oxidation of reactive azo  
588 dye with UV–H<sub>2</sub>O<sub>2</sub> process. *Dyes, and Pigments*, 62 (3), 269–275.  
589 <https://doi.org/10.1016/j.dyepig.2003.12.006>  
590

591 Nassar, M.Y., Moustafa, M.M., & Taha, M.M. (2016). Hydrothermal tuning of the morphology  
592 and particle size of hydrozincite nanoparticles using different counterions to produce  
593 nanosized ZnO as an efficient adsorbent for textile dye removal. *RSC Advances*, 6,  
594 42180–42195. <https://doi.org/10.1039/C6RA04855B>  
595

596 Ranfang, Z., Gaoxiang, D., Weiwei, Z., Lianhua, L., Yanming, L., Lefu, M., et al. (2014).  
597 Photocatalytic Degradation of Methylene Blue Using TiO<sub>2</sub> Impregnated Diatomite. *Advances*  
598 *in Materials Science and Engineering*, 2014, 1-7. <https://doi.org/10.1155/2014/170148>  
599

600 Rashad, M., Shaalan, N.M., & Abd-Elnaiem, A.M. (2016). Degradation enhancement of  
601 methylene blue on ZnO nanocombs synthesized by thermal evaporation technique.  
602 *Desalination and Water Treatment*, 57 (54), 26267–26273.  
603 <https://doi.org/10.1080/19443994.2016.1163511>  
604

605 Shen, S., Kronawitter, C., & Kiriakidis, G. J. (2017). An overview of photocatalytic materials.  
606 *Materiomics*,3(1), 1–2. <https://doi.org/10.1016/j.jmat.2016.12.004>  
607

608 Siong, V.L.E., Lee, K.M., Juan, J.C., Lai, C.W., Tai, X.H., & Khe, C.S. (2019). Removal of  
609 methylene blue dye by solvothermally reduced graphene oxide: a metal-free adsorption and  
610 photodegradation method. *RSC Advance*, 9 (64), 37686–37695.  
611 <https://doi.org/10.1039/C9RA05793E>  
612  
613

614 Sun, L., Hu, D., Zhang, Z., & Deng, X. (2019). Oxidative Degradation of Methylene Blue via  
615 PDS-Based Advanced Oxidation Process Using Natural Pyrite. *International Journal of*  
616 *Environmental Research and Public Health*, 16 (23), 4773.  
617 <https://doi.org/10.3390/ijerph16234773>  
618

619 Tang, L.-Z., Lin, Y.-L., Xu, B., Xia, Y., Zhang, T.-Y., Hu, C.-Y., et al. (2021). Photodegradation  
620 pathway of iodate and formation of I-THMs during subsequent chloramination in iodate-iodide-  
621 containing water. *Water Research*, 193, 116851.  
622 <https://doi.org/10.1016/j.watres.2021.116851>  
623

624 Velanganni, S., Pravinraj, S., Immanuel, P., & Thiruneelakandan, R. (2018). Nanostructure  
625 CdS/ZnO heterojunction configuration for photocatalytic degradation of Methylene blue.  
626 *Physica B: Condensed Matter*, 534 56-62. <https://doi.org/10.1016/j.physb.2018.01.027>

627  
628 Venkatraman, S.K., Saraswat, M., Choudhary, R., Senatov, F., Kaloshkin, S., & Swamiappan,  
629 S. (2020). Photocatalytic Degradation of Methylene Blue Dye by Calcium-and Magnesium-  
630 Based Silicate Ceramics. *ChemistrySelect*, 5 (39), 12198– 12205.  
631 <https://doi.org/10.1002/slct.202003046>  
632  
633 Wang, S. , Luo, C., Tan, F., Cheng, X., Ma, Q., Wu, D. et al. (2021). Degradation of Congo  
634 red by UV photolysis of nitrate: kinetics and degradation mechanism. *Separation and*  
635 *Purification Technology*, 262,118276. <https://doi.org/10.1016/j.seppur.2020.118276>  
636  
637 Wang, W.-L., Zhang, X., Wu, Q.-Y., Du, Y., Hu, & H.-Y. (2017). Degradation of natural organic  
638 matter by UV/chlorine oxidation: Molecular decomposition, formation of oxidation byproducts  
639 and cytotoxicity. *Water Research*, 124, 251-258. <https://doi.org/10.1016/j.watres.2017.07.029>  
640  
641 Wen, D., Li, W., Lv, J., Qiang, Z., & Li, M. (2019). Methylene blue Degradation by the  
642 VUV/UV/Persulfate Process: Effect of pH on the Roles of Photolysis and Oxidation. *Journal of*  
643 *Hazardous Materials*, 391, 121855. <https://doi.org/10.1016/j.jhazmat.2019.121855>  
644  
645 Wenhui, Q., Ming Z., Jing S., Yiqun, T., Meijuan, F., Yi, Z., Ting Z., et al. (2019). Photolysis of  
646 enrofloxacin, pefloxacin and sulfaquinoxaline in aqueous solution by UV/H<sub>2</sub>O<sub>2</sub>, UV/Fe(II), and  
647 UV/H<sub>2</sub>O<sub>2</sub>/Fe(II) and the toxicity of the final reaction solutions on zebrafish embryos. *Science*  
648 *of the Total Environment*, 651, 1457–1468. <https://doi.org/10.1016/j.scitotenv.2018.09.315>  
649  
650 Xu, C., Sun, Y., Liu, J., Guo, L., & Zhou, X. (2024). Optimizing orange II wastewater treatment:  
651 Unveiling the catalytic potential of nitrate and iodide ions in ultraviolet photolysis. *Journal of*  
652 *Water Process Engineering*, 64,105677. <https://doi.org/10.1016/j.jwpe.2024.105677>  
653  
654 Yang, C., Dong, W., Cui, G., Zhao, Y., Shi, X., Xia, X., et al. (2017). Highly efficient  
655 photocatalytic degradation of methylene blue by P2ABSA-modified TiO<sub>2</sub> nanocomposite due  
656 to the photosensitization synergetic effect of TiO<sub>2</sub> and P2ABSA. *RSC Advance*. 7, 23699.  
657 <https://doi.org/10.1039/C7RA02423A>  
658  
659 Zhang, L.C<sup>a</sup>; Jia, Z.; Lyu, F.; Liang, S.X.; Lu, J. (2019). A review of catalytic performance of  
660 metallic glasses in wastewater treatment: Recent progress and prospects. *Progress in*  
661 *Materials Science*, 105, 100576. <https://doi.org/10.1016/j.pmatsci.2019.100576>  
662  
663 Zhang, F.<sup>b</sup>, Wang, X., Liu, H., Liu, C., Wan, Y., Yunze Long, Y., & Cai, Z. (2019). Recent  
664 Advances and Applications of Semiconductor Photocatalytic Technology. *Applied sciences*,  
665 9(12), 2489. <https://doi.org/10.3390/app9122489>  
666  
667  
668 Zhiquan, L., Congwei, L., Fengxun, T., Daoji, W., Xuedong, Z., Shishun, W., et al. (2022).  
669 UV light irradiation combined with nitrate f or degradation of bisphenol A: kinetics,  
670 transformation pathways, and acute toxicity assessment. . *Environmental Science: Water*  
671 *Research & Technology*, 8(3) 586-596. <https://doi.org/10.1039/D1EW00796C>  
672  
673  
674  
675  
676  
677  
678  
679